FULL PAPER

Internal Medicine

Long-term administration of prednisolone: Effects on the myocardial tissue of healthy beagle dogs

Sachiyo TANAKA[1)]*, Hitomi SHIBUYA[1)], Shuji SUZUKI[1)], Nobuo KANNO[1)], Yasuji HARADA[1)], Asaka SATO[2)], Satoshi SOETA[3)] and Yasushi HARA[1)]

[1)]Division of Veterinary Surgery, Department of Veterinary Science, Faculty of Veterinary Medicine, Nippon Veterinary and Life Science University, 1-7-1 Kyonan, Musashino, Tokyo 180-8602, Japan

[2)]Azabu University Veterinary Teaching Hospital, Soft Tissue and Tumor Surgery, 1-17-71 Fuchinobe, Chuo, Sagamihara, Kanagawa 252-5201, Japan

[3)]Division of Veterinary Anatomy, Department of Veterinary Science, Faculty of Veterinary Medicine, Nippon Veterinary and Life Science University, 1-7-1 Kyonan, Musashino, Tokyo 180-8602, Japan

ABSTRACT. This study aimed to assess the structural and functional effects of long-term hyperglucocorticoidemia on canine myocardium and compare these parameters with histopathological changes. Twelve healthy male beagle dogs were enrolled and assigned to the high-dose prednisolone (P; n=6) and control (C; n=6) groups. The P group was treated with 2 mg/kg of prednisolone BID for 84 days. Clinical parameters were measured using echocardiography and non-invasive systolic blood pressure (SBP) measured before the initiation of synthetic corticosteroids and at 7, 28, 56, and 84 days after the start of medication. For histological evaluation, cardiovascular tissue was harvested from dogs in groups P (at the end of the medication period) and C (scheduled to be euthanized for unrelated reasons). In the P group, clinical changes including thickening of the left ventricular free wall (LVFW) and interventricular septum (IVS), decreased left ventricular (LV) diastolic function, and increased SBP were observed after the start of medication. During histological evaluation, fibrosis was observed in the LVFW and IVS in the P group. Furthermore, decreased glucocorticoid receptor (GCR) levels were observed in the LVFW, right ventricular free wall (RVFW), and IVS and increased mineralocorticoid receptor (MCR) levels were observed in the LVFW and RVFW in the P group compared with those in the C group. In conclusion, fibrosis may cause LV structural and functional abnormalities in dogs with hyperadrenocorticism. Furthermore, GCR downregulation and upregulated MCR might influence the myocardial fibrosis.

KEY WORDS: canine, Cushing syndrome, diastolic dysfunction, fibrosis, left ventricular hypertrophy

In 2009, the incidence of Cushing syndrome (CS) in dogs was reported to be 1–2 cases/1,000 dogs/year, making it a common endocrine disorder in dogs [13]; CS causes systemic changes such as polyuria, polyphagia, skin lesions, including hair loss, abdominal distention, and panting due to hypercortisolemia [3, 35]. In human patients with CS, as in dogs, the overproduction of cortisol causes systemic changes including abdominal distention, hypertension, and abnormal glucose tolerance [4, 34]. Cardiovascular complications in human patients with CS cause a 4-fold higher mortality rate than in the healthy population, indicating that systemic changes in CS are associated with cardiovascular risk [4, 33]. The presence of left ventricular hypertrophy (LVH) and diastolic dysfunction (DD) has been reported in patients with CS [24, 33]. Furthermore, cardiomyocyte hypertrophy and increased myocardial fibers have been reported as histopathological changes in the heart [25, 30, 43]. Recently, in veterinary medicine, LVH and DD have been reported in dogs with CS and those receiving high-dose prednisolone [9, 22, 44]. To our knowledge, current experimental studies on dogs are short-term evaluations [22, 32, 45] that report no obvious histopathological myocardial changes [22]. In other words, the etiology of hyperglucocorticoidemia (HGC) causing LVH and DD in dogs remains elusive. Therefore, we investigated the causes of LVH and DD in dogs, by evaluating the structural and functional effects of long-term HGC on the myocardium and comparing these parameters with histopathological changes.

*Correspondence to: Tanaka, S.: sachiyoct@gmail.com

MATERIALS AND METHODS

Animals

Twelve healthy male research beagle dogs were recruited for this study. Six dogs (weight: 9.5–11.2 kg, median weight: 10.8 kg, age: 15–17 months, median age: 16.0 months) in the high-dose prednisolone group (P group) were orally administered a synthetic corticosteroid, at a dose of 2 mg/kg (5 mg prednisolone tablet "YD", Yoshindo Co., Ltd., Toyama, Japan) every 12 hr for 84 days. Clinical parameters of the P group included physical examination, complete blood count (CBC), blood biochemistry, electrocardiography, non-invasive blood pressure measurements, and echocardiography conducted before the initiation of medication (Day 0) and at 7, 28, 56, and 84 days after the start of medication (Day 7, Day 28, Day 56, Day 84). At Day 0-examination, all six dogs in the P group were carefully identified as healthy with no evidence of systemic or cardiac disease or congenital abnormalities of the heart. At each test point after the start of medication, the patient's general condition was confirmed to not interfere with the continuation of the experiment (for example, no blood parameters and clinical findings were available to suspect pancreatitis or infection, and no evidence of body surface lacerations was present), and changes over time were evaluated. Moreover, on Day 0 and Day 84, ACTH stimulation tests were performed through intramuscular administration of tetra-cosactide (0.25 mg Cortrosyn injection, Daiichi Sankyo Co., Ltd., Tokyo, Japan) (125 μg for dogs <5 kg or 250 μg for dogs >5 kg) and obtaining baseline and 1-hr post-injection blood samples [35]. Serum cortisol concentrations were measured using the chemiluminescence enzyme immunoassay method (Fuji Film, Monolith, Tokyo, Japan). At Day 84, dogs in the P group were euthanized with pentobarbital (Kyoritsu Seiyaku, Tokyo, Japan; 90 mg/kg, intravenously) for histopathological examination. Six healthy male study beagle dogs (weight: 8.5–10.5 kg, median weight: 9.6 kg, age: 8–19 months, median age: 17.5 months) were used in the control group (C group), which were euthanized in the same procedure for other purposes; dogs in the C group were preliminarily examined by physical and electrocardiographic examination and blood pressure measurements to ensure that they were free of abnormalities. This study was approved by the Laboratory Animal Committee of the Nippon Veterinary and Life Science University (approval number: 29S-37), and all dogs were handled and treated according to the laboratory animal guidelines of the Nippon Veterinary and Life Science University.

Systolic blood pressure measurement

Blood pressure was measured using an oscillometric automatic blood pressure monitor (Blood pressure monitor for animals BP100, Fukuda M-E Kogyo Co., Ltd., Tokyo, Japan) [11]. Blood pressure was measured according to The American College of Veterinary Internal Medicine guidelines for SBP measurement [5]. With the dog in a supine, gently restrained position, an inflatable cuff was wrapped under the right hind tarsal joint, and measurements were taken in a quiet, isolated room with a 10 min acclimation time for each measurement day. The selected cuff width was approximately 40% of the circumference of the measurement site. The initial results were discarded, and the mean values of systolic blood pressure (SBP) and heart rate measured over three subsequent sessions were used as measurements. In the current study, systemic hypertension (SHT) was defined as SBP greater than 160 mmHg [11, 44].

Echocardiography

Echocardiography was performed by Tanaka using a diagnostic ultrasound device (Vivid E95, GE Healthcare UK Ltd., Little Chalfont, Buckinghamshire, UK). Echocardiography was performed without sedation or anesthesia, with the dog in a supine, gently restrained position. A Sector probe (6S probe, GE Healthcare UK Ltd.) was used for all tests. All recorded images were measured using the same diagnostic ultrasound device, and the mean values in three consecutive heartbeats were used as the measurement value.

Conventional echocardiography

In the B-mode LV short-axis view at the level of the papillary muscle, parameters including interventricular septum end-diastole (IVSd), interventricular septum end-systole (IVSs), left ventricular free wall end-diastole (LVFWd), left ventricular free wall end-systole (LVFWs), left ventricular internal diameter end-diastole (LVIDd), and left ventricular internal diameter end-systole (LVIDs) were measured using the leading edge-to-leading edge method [42]. The ejection fraction (EF) and fractional shortening were calculated. To assess left ventricular (LV) remodeling, relative wall thickness (RWT), and LV mass (LVM) were calculated [17]. The following formulas were used to calculate, respectively; RWT=(IVSd + LVFWd)/ LVIDd, LVM=$0.8 \times (1.04 \times (LVId + LVFWd + IVSd)^3 - (LVIDD)^3 + 0.6$ [19]. In the right parasternal LV short-axis view at the level of the heart base, the left atrial to aortic diameter ratio (LA/AO) was determined through the endocardial-cavity interface method. In brief, the internal diameter of the AO was determined along the commissure between the noncoronary and right coronary aortic valve cusp, and the internal diameter of the LA was determined along a line extending from and parallel to the commissure between the noncoronary and left coronary aortic valve cusp to the distant margin of the LA on the 1st frame after aortic valve closure [39]. A sample of 2-mm width was used to determine the blood flow velocity. In the left apical 4-chamber view, the early diastolic wave of transmitral flow peak velocity (E vel), the duration of deceleration of the early diastolic wave of transmitral flow (E decel time) and the systolic atrial wave of transmitral flow peak velocity (A vel) were measured by pulsed-doppler mode, and the ratio of the early diastolic to systolic atrial wave transmitral flow peak velocity (E/A) was calculated. From the left apical 5-chamber view, the aortic peak velocity (AO vel), the ratio of the pre-ejection period and ejection time (PEP/ET), the isovolumic contraction time (ICT) and the isovolumic relaxation time (IRT) were determined. PEP was measured as the time from the beginning of the Q wave on the

electrocardiogram to the beginning of LV ejection, and ET was measured as the time from the beginning to the end of the AO doppler flow signal [28]. Besides, ICT was measured as the period from the end of the A vel doppler flow signal to the beginning of the AO doppler flow signal, and IRT was measured as the period from the end of the AO doppler flow signal to the beginning of the E vel doppler flow signal.

Tissue doppler imaging

The color doppler imaging method was used for Tissue doppler imaging (TDI) to minimize the time of canine restraint [48]. To avoid artifacts due to aliasing, the velocity range was adjusted to allow measurement of maximum myocardial velocity. Position and size adjustment of the region of interest (ROI) was performed in all cases to ensure that the ROI remained within the myocardium throughout the cardiac cycle [48]. Peak velocities of LV myocardium at systole (Sm), peak velocities of LV myocardium at early diastole (Em), and peak velocities of LV myocardium at atrial systole (Am) were measured at the mitral valve annulus of the left apical four-chamber view on the IVS and LVFW sides, respectively.

Histological examination

Dogs in groups C and P had their hearts and aortic bases taken promptly after euthanasia. Subsequently, the heart was cut at the incision line using a sharp disposable blade so that the midpoint of the incision line from the coronal groove to the apex of the heart was parallel to the coronal groove. After incision of the heart, aortic base, and the left ventricular free wall (LVFW), right ventricular free wall (RVFW) and interventricular septum (IVS) were incised and immersed in 4% paraformaldehyde (PFA) in 0.1 M phosphate buffer (pH 7.4). The process up to this point was carried out within 30 min after euthanasia in all animals. The tissues were then immersed in PFA for 24 hr and fixed, and the tissue specimens were embedded in paraffin according to the normal method and thinly sliced to a thickness of 3 µm. The sections were then stained for hematoxylin and eosin (HE), phosphotungstic acid-hematoxylin (PTAH), and Masson's trichrome (MT) according to conventional methods. PTAH staining was performed at sites other than the aorta; meanwhile, HE and MT stained the aorta in the tunica media and internal areas. Tissue sections stained with HE and PTAH were evaluated by Tanaka, S and Soeta, S, respectively, blinded to group classification. In MT-stained sections, three randomly selected fields per tissue section were photographed using a digital microscope camera (DP71; OLYMPUS, Tokyo, Japan) at 200× magnification. The percentage of collagen fiber regions stained with aniline blue was calculated using image analysis software (ImageJ; version 1.43u, National Institutes of Health, Washington, DC, USA). The mean values of each of the three visual fields were calculated.

Immunohistochemical examination

After deparaffinization, tissue sections were immersed in 1% hydrogen peroxide (H_2O_2) for 30 min to block endogenous peroxidase activity. After washing with phosphate-buffered saline (PBS), to retrieve target antigens, anti-glucocorticoid receptor (GCR) immunostained sections were incubated with citrate buffer (0.01 M, pH 6.0) for 60 min at 60°C [27]. Anti-mineralocorticoid receptor (MCR) immunostained sections were microwaved with tris-ethylenediaminetetraacetic acid (EDTA) buffer (10 mM tris, 1 mM EDTA, pH 9.0) for 15 min at an output of 500 W. The sections were then cooled at room temperature for 30 min. After washing with PBS, the sections were treated with 10% normal goat serum (Nichirei Biosciences Inc., Tokyo, Japan) for 30 min. In this blocking treatment, the anti-GR receptor immunostained sections were treated with 10% normal goat serum diluted 1,000 times. Subsequently, the sections for GCR and MCR staining were incubated overnight at room temperature with an anti-GCR rabbit polyclonal antibody (1:1,000, Abcam, Cambridge, UK) and anti-MCR mouse monoclonal antibody (1:1,000, Abcam), respectively. Sections were washed with PBS and then incubated with a peroxidase-conjugated antibody to rabbit immunoglobulin (Simple Stain Rat MAX-PO (MULTI), Nichirei Biosciences Inc.) for 1 hr at room temperature. After sections were rewashed with PBS, colored with DAB chromogen solution (Histofine DAB Substrate Kit, Nichirei Biosciences Inc.), and counterstained with hematoxylin.

Three randomly selected fields of view per section were photographed and evaluated for positive anti-GCR immunopositive nuclei and MCR immunoreactive sites in the myocardium and aorta at a magnification of 400×. Moreover, the mean values of each of the three visual fields were calculated. At the time of photography and evaluation of tissue sections, group classification was blinded.

Statistical analysis

The Shapiro-Wilk test was performed to assess normality for weight, age, blood tests, and other continuous data and denoted as median (range). The clinical data were analyzed using univariate mixed-effect linear regression for the change over time in each parameter at Day 0, Day 7, Day 28, Day 56, and Day 84. The outcome variables were clinical data (including SBP) obtained continuously at each measurement point and independent variables including time, weight, age, and SBP. The fixed effect was time. Dog identities were considered the random effect.

Histological data were analyzed through univariate linear regression analysis for the C and P groups. The results of histological analysis were the outcome variable, and the independent variables were groups, clinical data, weight, and age. The fixed effects were groups (the C and P groups).

Stata/IC 14.0 (StataCorp, College Station, TX, USA), a commercially available statistical software, was used for all analyses. Statistical estimates and inferences were performed with two-tailed hypotheses and tests at the 5% significance level, and the coefficient (Co), 95% confidence interval (CI), and *P*-value (*P*) were determined. The Wald test was used to assess the validity of

the effect of the independent variables in linear regression with respect to their significance, and the validity of the fitted model. The residual plot was generated after fitting the regression model to assure linearity of the relationship of the outcome variable and independent variable. Tukey's HSD test was performed for the *post-hoc* pairwise comparison.

RESULTS

Clinical parameters

The clinical signs in the P group included polyuria, which appeared a few days after the start of the medication. The CBC results showed a significant increase in neutrophilic white blood cell count after Day 7. In addition, blood biochemistry results showed an increase in triglycerides after Day 7 and an increase in alanine aminotransferase, alkaline phosphatase, and γ-glutamyl transpeptidase at Day 84 (data not shown). For the ACTH stimulation test, baseline and post-stimulation serum cortisol concentrations at Day 0 were within the normal range, and the response of serum cortisol concentrations was observed in post-stimulation. In contrast, baseline and post-stimulation serum cortisol concentrations at Day 84 were low or within the normal range, and no response was observed in post-stimulation (Table 1). SBP at Day 84 was significantly increased compared with Day 0 measurements (Co=30.208; CI=14.608–45.809; *P*<0.0001); 3 dogs met the definition of SHT, exceeding 160 mmHg (Table 1).

Conventional echocardiography

The evolution of parameters on general echocardiography in the P group is shown in Table 2. Compared with the measurements of Day 0, there was a significant increase in IVSd and IVSs at Day 56 (Co=1.580; CI=0.587–2.573; *P*=0.002, and Co=2.353; CI=0.626–4.081; *P*=0.008, respectively) and Day 84 (Co=1.683; CI=0.690–2.676; *P*=0.001, and Co=2.158; CI=0.431–3.886; *P*=0.014, respectively). There was also a significant increase in LVFWd and LVFWs at Day 56 (Co=0.767; CI=0.113–1.421; *P*=0.022, and Co=2.165; CI=0.690–3.640; *P*=0.004, respectively) and LVFWs at Day 84 (Co=1.520; CI=0.045–2.995; *P*=0.043). The LVFWd did not significantly increase on Day 84 compared with that on Day 0 (*P*=0.080). Throughout the medication period, there was no significant change in LVIDd or LVIDs. For EF, there was a significant increase only at Day 56 compared with Day 0 measurements (Co=9.835; CI=0.256–19.414; *P*=0.044). Compared to measurements at Day 0, the following was observed: for LVM, a significant increase at Day 28 (Co=10.505; CI=3.316–17.694; *P*=0.004), Day 56 (Co=19.182; CI=11.993–26.371; *P*<0.0001), and Day 84 (Co=14.414; CI=7.225–21.603; *P*<0.0001); for RWT, a significant increase at Day 84 (Co=0.064; CI=0.002–0.125; *P*=0.043); for AO vel, a significant increase at Day 28 (Co=0.270; CI=0.053–0.487; *P*=0.015); for PEP/ET, a significant increase at Day 84 (Co=0.087; CI=0.033–0.141; *P*=0.001); for E vel, a significant increase at Day 56 (Co=17.222; CI=0.785–33.659; *P*=0.040); for A vel, a significant increase at Day 28 (Co=17.500; CI=3.794–31.206; *P*=0.012), Day 56 (Co=22.222; CI=8.516–35.928; *P*=0.001), and Day 84 (Co=16.442; CI=2.736–30.148; *P*=0.019); there was no significant change in the E decel time, E/A ratio, ICT and IRT. In conventional echocardiography, no significant relationships with SBP were found for all items.

Tissue doppler imaging

The changes in parameters in TDI in the P group are shown in Table 3. For IVS side Em, there was a significant decrease at Day 28 (Co=−1.015; CI=−1.935–−0.095; *P*=0.031), Day 56 (Co=−1.602; CI=−2.522–−0.681; *P*=0.001), and Day 84 (Co=−1.272; CI=−2.192–−0.351; *P*=0.007) compared with Day 0 measurements. Moreover, there was a significant decrease in IVS side Em/Am at Day 28 compared with Day 0 measurements (Co=−0.509; CI=−0.780–−0.031; *P*=0.008), and a significant increase in IVS side E/Em at Day 28 (Co=4.533; CI=0.405–8.661; *P*=0.031), Day 56 (Co=9.338; CI=5.210–13.466; *P*<0.0001), and Day 84 (Co=6.779; CI=2.651–10.907; *P*=0.001). On the LVFW side, there was a significant increase in E/Em at Day 28 (Co=0.089; CI=0.019–0.159; *P*=0.013), Day 56 (Co=0.107; CI=0.037–0.177; *P*=0.003), and Day 84 (Co=0.073; CI=0.003–0.143; *P*=0.041). For Sm, there was a significant increase at Day 28 (Co=1.578; CI=0.005–3.152; *P*=0.049), Day 56 (Co=2.058; CI=0.485–3.632; *P*=0.010), and Day 84 (Co=2.048; CI=0.476–3.622; *P*=0.011) on the IVS side, and at Day 28 (Co=2.153; CI=0.712–3.595; *P*=0.003) and Day 56 (Co=1.670; CI=0.228–3.112; *P*=0.023) on the LVFW side. For TDI, a negative relationship with SBP was found on the IVS side Em (Co=−0.024; CI=0.044–0.004; *P*=0.019), while a positive relationship was found on the IVS side Sm (Co=0.044; CI=0.011–0.077; *P*=0.009).

Table 1. Medians and ranges of clinical parameters in the high-dose prednisolone group

	Median				
	Day 0	Day 7	Day 28	Day 56	Day 84
Pre-ACTH serum Cortisol concentration (μg/dl)	2.7 (1.1–4.4)				2.2 (0.5–3.7)
Post-ACTH serum Cortisol concentration (μg/dl)	9.8 (5.0–12.5)				1.5 (0.5–2.2)
Heart rate (bpm)	140 (90–169)	118 (63–166)	128 (89–195)	121 (102–180)	124 (91–154)
SBP (mmHg)	139 (127–152)	155 (130–168)	153 (135–174)	148 (132–172)	161** (155–202)

ACTH: adrenocorticotropic hormone; bpm: beats per minute; Day 0: Before initiation of medication; Day 7: 7 days after the initiation of medication; Day 28: 28 days after the initiation of medication; Day 56: 56 days after the initiation of medication; Day 84: 84 days after the initiation of medication; SBP: systolic blood pressure. Data are expressed as medians (range). **Indicates a significant difference compared to Day 0 values at *P*<0.01. The reference ranges of the baseline plasma cortisol concentration and the post-stimulation plasma cortisol concentration were 1.0–7.8 μg/dl and 5.0–20.0 μg/dl, respectively [40].

Table 2. Conventional echocardiographic parameters in the high-dose prednisolone group

	Median				
	Day 0	Day 7	Day 28	Day 56	Day 84
B-mode					
IVSd (mm)	7.77 (5.81–9.43)	7.81 (6.97–10.99)	9.10 (6.80–9.69)	9.64** (7.78–11.18)	9.50** (8.18–10.80)
IVSs (mm)	11.67 (8.20–13.70)	12.83 (9.40–18.40)	12.70 (10.60–15.20)	13.32** (11.80–15.40)	13.25* (10.90–15.60)
LVFWd (mm)	7.64 (5.49–10.45)	7.85 (5.67–9.73)	7.44 (6.23–10.31)	8.32* (6.91–10.88)	8.34 (6.64–11.11)
LVFWs (mm)	12.02 (9.80–13.20)	13.33 (11.30–16.30)	12.79 (10.40–16.90)	14.09** (10.20–16.60)	12.72* (11.80–15.90)
LVIDd (mm)	30.86 (25.44–34.65)	31.82 (27.22–34.22)	31.82 (28.92–35.06)	31.37 (28.66–35.34)	31.04 (28.34–32.47)
LVIDs (mm)	19.97 (12.26–24.06)	17.74 (9.62.–24.32)	19.16 (14.54–23.51)	18.08 (12.97–23.90)	18.64 (14.64–25.47)
EF (mm)	68.50 (33.96–84.74)	76.57 (50.54–93.22)	72.66 (52.97–84.12)	77.55* (60.17–87.35)	71.98 (40.57–86.13)
FS (mm)	38.13 (15.42–51.92)	44.13 (24.88–64.55)	41.06 (26.33–51.68)	45.16 (31.28–55.52)	40.00 (19.07–54.25)
RWT	0.54 (0.43–0.55)	0.50 (0.42–0.61)	0.51 (0.48–0.60)	0.54 (0.49–0.65)	0.55* (0.51–0.67)
LVM (g)	61.88 (42.42–71.03)	63.64 (57.04–74.57)	69.40** (52.86–86.92)	80.12** (64.47–88.19)	71.31** (58.76–87.35)
LA/AO	1.08 (0.94–1.24)	1.07 (0.88–1.30)	1.15 (0.93–1.37)	1.11 (1.04–1.39)	1.13 (0.77–1.47)
Pulse-doppler- mode					
E velocity (cm/sec)	97.5 (78.0–133.0)	98.8 (89.0–110.0)	103.5 (91.0–155.0)	116.3* (111.0–125.0)	113.0 (106.0–121.0)
E decel time (msec)	99.88 (62.35–109.70)	81.15 (66.95–101.19)	98.66 (74.47–113.65)	90.55 (79.24–108.02)	80.50 (71.36–95.72)
A velocity (cm/sec)	57.2 (41.0–82.0)	62.7 (51.0–84.0)	72.8* (52.0–109.0)	85.0** (60.0–94.0)	76.2* (59.0–89.0)
E/A	1.63 (1.31–2.43)	1.58 (1.32–2.00)	1.46 (1.24–1.93)	1.41 (1.24–1.91)	1.50 (1.24–1.82)
AO velocity (m/sec)	1.45 (0.84–1.62)	1.38 (1.20–1.56)	1.59* (1.40–1.96)	1.43 (1.39–1.73)	1.45 (1.13–1.69)
PEP/ET	0.40 (0.23–0.43)	0.38 (0.34–0.43)	0.35 (0.31–0.47)	0.37 (0.26–0.53)	0.46* (0.37–0.50)
ICT (msec)	38.50 (28.55–68.51)	37.13 (28.50–48.20)	39.96 (19.98–45.00)	37.10 (20.42–43.01)	31.63 (22.83–62.80)
IRT (msec)	49.95 (28.54–68.50)	38.54 (25.49–48.53)	38.46 (25.69–51.12)	39.96 (34.25–52.80)	37.11 (28.55–45.67)

A: atrial systolic wave of transmitral flow velocity; AO: Aortic; Day 0: Before initiation of medication; Day 7: 7 days after the initiation of medication; Day 28: 28 days after the initiation of medication; Day 56: 56 days after the initiation of medication; Day 84: 84 days after the initiation of medication; E: early diastolic wave of transmitral flow; E decel time: deceleration time of early diastolic wave of transmitral flow, E/A: early diastolic to atrial systolic wave transmitral flow velocity; EF: ejection fraction; FS: fractional shortening; ICT: isovolumic contraction time; IRT: isovolumic relaxation time; IVSd: interventricular septal thickness in end-diastole; IVSs: interventricular septal thickness in end-systole; LA/AO: left atrium to aorta ratio; LVFWd: left ventricular free wall thickness in end-diastole; LVFWs: left ventricular free wall thickness in end-systole; LVIDd: left ventricular end-diastolic diameter; LVIDs: left ventricular end-systolic diameter; LVM: LV mass; PEP/ET: pre-ejection period and ejection time; RWT: relative wall thickness. Data are expressed as medians (range). * and ** Indicate significant difference compared to Day 0 values at *P*<0.05 and *P*<0.01, respectively.

Table 3. Tissue velocity imaging parameters of the mitral annulus in the high-dose prednisolone group

Tissue-doppler-mode	Median				
	Day 0	Day 7	Day 28	Day 56	Day 84
IVS velocity					
Sm (cm/sec)	6.89 (4.34–8.44)	6.51 (5.45–10.18)	8.57* (5.25–10.46)	9.06* (7.28–10.14)	9.06* (7.52–10.27)
Em (cm/sec)	6.12 (4.64–7.27)	5.72 (3.27–7.42)	5.15* (4.86–5.41)	4.62** (3.77–5.65)	4.92** (4.32–5.61)
Am (cm/sec)	3.80 (2.97–5.99)	3.76 (1.76–5.63)	4.65 (3.65–6.42)	4.75 (3.53–5.27)	4.39 (2.71–5.99)
Em/Am	1.46 (1.20–1.94)	1.72 (0.91–2.58)	1.11* (0.80–1.42)	0.98 (0.76–1.31)	1.17 (0.74–1.59)
E/Em	6.37 (11.88–23.11)	7.86 (12.22–27.22)	10.88* (17.19–28.71)	12.54** (20.77–31.39)	10.92** (19.31–28.30)
LVFW velocity					
Sm (cm/sec)	7.29 (4.93–10.43)	9.13 (6.57–10.27)	10.20* (8.27–10.54)	10.07 (6.83–10.56)	10.05 (5.89–10.52)
Em (cm/sec)	5.65 (4.36–9.52)	7.12 (4.05–9.15)	7.15 (6.00–9.06)	6.52 (3.23–8.24)	5.08 (2.51–7.32)
Am (cm/sec)	3.81 (2.87–7.48)	4.70 (2.67–7.03)	5.17 (4.53–7.36)	4.75 (2.92–6.62)	5.11 (3.3–7.15)
Em/Am	1.40 (0.94–2.15)	1.44 (1.30–2.06)	1.39 (0.95–2.00)	1.14 (0.87–2.74)	0.92 (0.66–1.61)
E/Em	4.60 (8.97–20.30)	5.94 (10.65–23.87)	6.00* (10.92–22.29)	7.62** (14.26–38.70)	11.45* (14.80–47.54)

Am: peak velocities of left ventricular myocardium at late diastole; Day 0: Before initiation of medication; Day 7: 7 days after the initiation of medication; Day 28: 28 days after the initiation of medication; Day 56: 56 days after the initiation of medication; Day 84: 84 days after the initiation of medication; Em: peak velocities of left ventricular myocardium at early diastole; IVS: interventricular septal; LVFW, left ventricular free wall; Sm: peak velocities of left ventricular myocardium at systole. Data are expressed as medians (range). * and ** Indicate significant difference compared to Day 0 values at *P*<0.05 and *P*<0.01, respectively.

Histological examination and immunohistochemical examination

There were no significant differences in age or weight between the two groups evaluated histologically (the C group and the P group).

HE-stained tissues showed no abnormalities or detectable changes in any of the samples of the C or P groups. PTAH-stained myocardium showed no detectable changes in myocardial transverse striations in the C or P groups.

MT staining revealed blue-stained collagen fibers at the intramyocardial spaces and media of the aorta in the C and P groups. More

collagen fibers appeared to be detected in the P group than in the C group, especially in the LVFW and IVS (Fig. 1).

Quantitative evaluation using image analysis software showed that the LVFW and IVS of the P group showed a significantly higher percentage of collagen fibers compared with those of the C group (Co=0.398; CI=0.113–0.682; P=0.006, and Co=0.170; CI=0.039–0.302; P=0.011, respectively; Table 4). For MT staining results, no significant relationship with SBP was found for all parts under investigation. GCR immunoreactivity was detected in cardiomyocyte nuclei in the myocardium, with brown staining in both C and P groups, with fewer nuclei stained in the P group. In the aorta, the expression of GCR immunoreactive nuclei was low in both groups (Fig. 2). The percentage of GCR immunostaining-positive nuclei in the P group was significantly lower in the LVFW and RVFW (Co= −2.715; CI= −3.481– −1.950; P<0.0001, and Co= −1.941; CI= −3.184– −0.697; P=0.002, respectively) and ventricular septum (Co= −3.550; CI= −5.088– −2.011; P<0.0001) compared with that in the C group (Table 4). MCR immunoreactivity was detected in the cytoplasm and nuclei of cardiomyocytes, and brown granules were found in both the C group and the P group (Fig. 2). In the P group, the percentage of MCR immunostaining-positive sites in the LVFW and RVFW were significantly higher than those in the C group (Co=0.023; CI=0.004–0.042; P=0.016, and Co=0.048; CI=0.023–0.074; P<0.0001, respectively). In the IVS, no significant difference was observed between the two groups (P=0.100). In 12 dogs, there was a significant negative relationship between the percentage of area occupied by collagen fibers and the percentage of GCR immunostained positive nuclei with respect to the LVFW (Co= −0.155; CI= −0.236– −0.073; P<0.0001) and IVS (Co= −0.039; CI= −0.063– −0.014; P=0.002). In the LVFW, there was a significant negative relationship between the percentage of GCR immunostaining-positive nuclei and the percentage of MCR immunostaining-positive sites (Co= −0.008; CI= −0.014– −0.001; P=0.019). A significant positive relationship was observed between the percentage of area occupied by collagen fibers in the IVS and IVSd on echocardiographic results (Co=0.067; CI=0.071–0.127; P=0.028). Additionally, a significant positive relationship was observed between the percentage of area occupied by collagen
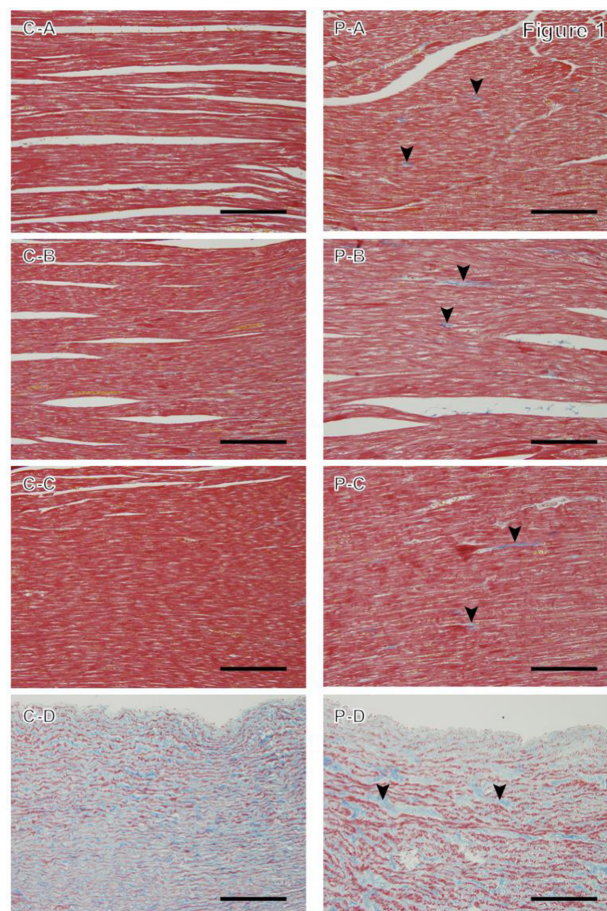

Fig. 1. Masson's trichrome staining in the control group (C) and high-dose prednisolone group (P). A: Myocardium of the left ventricular wall; B: myocardium of the right ventricular wall; C: interventricular septum; and D: aorta. The P group shows collagen fibers as thin fibrous structures stained blue at the intramyocardial spaces (arrowheads). Magnification: 200×, scale bar=100 μm.

Table 4. Comparison of collagen fibers, glucocorticoid receptor-positive nuclei, and mineralocorticoid receptor-immunoreactive areas between the two groups

	Percentage of collagen fibers		Percentage of GCR-positive nuclei		Percentage of MCR-immunoreactive areas	
	C group (%)	P group (%)	C group (%)	P group (%)	C group (%)	P group (%)
LVFW	0.83×10^{-1} $(0.57–5.34 \times 10^{-1})$	5.43×10^{-1}** $(0.34–9.78 \times 10^{-1})$	3.17 (2.53–4.32)	0.31** (0.00–2.10)	2.57×10^{-3} $(0.34–9.0 \times 10^{-3})$	20.03×10^{-3}* $(5.00–73.33 \times 10^{-3})$
RVFW	3.59×10^{-1} $(1.59–29.1 \times 10^{-1})$	4.91×10^{-1} $(0.14–8.17 \times 10^{-1})$	2.40 (1.21–4.85)	0** (0.00–2.64)	0.21×10^{-3} $(0.06–16.67 \times 10^{-3})$	49.67×10^{-3}** $(7.00–94.33 \times 10^{-3})$
IVS	1.48×10^{-1} $(0.92–2.30 \times 10^{-1})$	3.82×10^{-1}* $(0.63–4.72 \times 10^{-1})$	3.48 (0.99–7.25)	0.27** (0.00–0.67)	1.86×10^{-3} $(0.67–39.33 \times 10^{-3})$	20.67×10^{-3} $(3.33–35.67 \times 10^{-3})$
Aorta	20 (13.67–32.94)	26.94 (11.68–39.65)	0.13×10^{-3} $(0.00–1.67 \times 10^{-3})$	0 $(0.00–1.03 \times 10^{-3})$	0.98×10^{-3} $(0.17–2.69 \times 10^{-3})$	1.05×10^{-3} $(0.07–1.67 \times 10^{-3})$

C group: control group; GCR: glucocorticoid receptor; IVS: interventricular septal; LVFW: left ventricular free wall; MCR: mineralocorticoid receptor; P group: high-dose prednisolone group; RVFW: right ventricular free wall. For each tissue section, the area of collagen fibers stained with aniline blue was measured in three randomly selected visual fields at 200× magnification. For three randomly selected fields at 400× magnification, the number of GCR-positive and GCR-negative nuclei were counted, and MCR immunostaining-positive sites were measured at fields of view. Data are expressed as medians (range). * and ** Indicate significant difference between the two groups at P<0.05 and P<0.01, respectively.
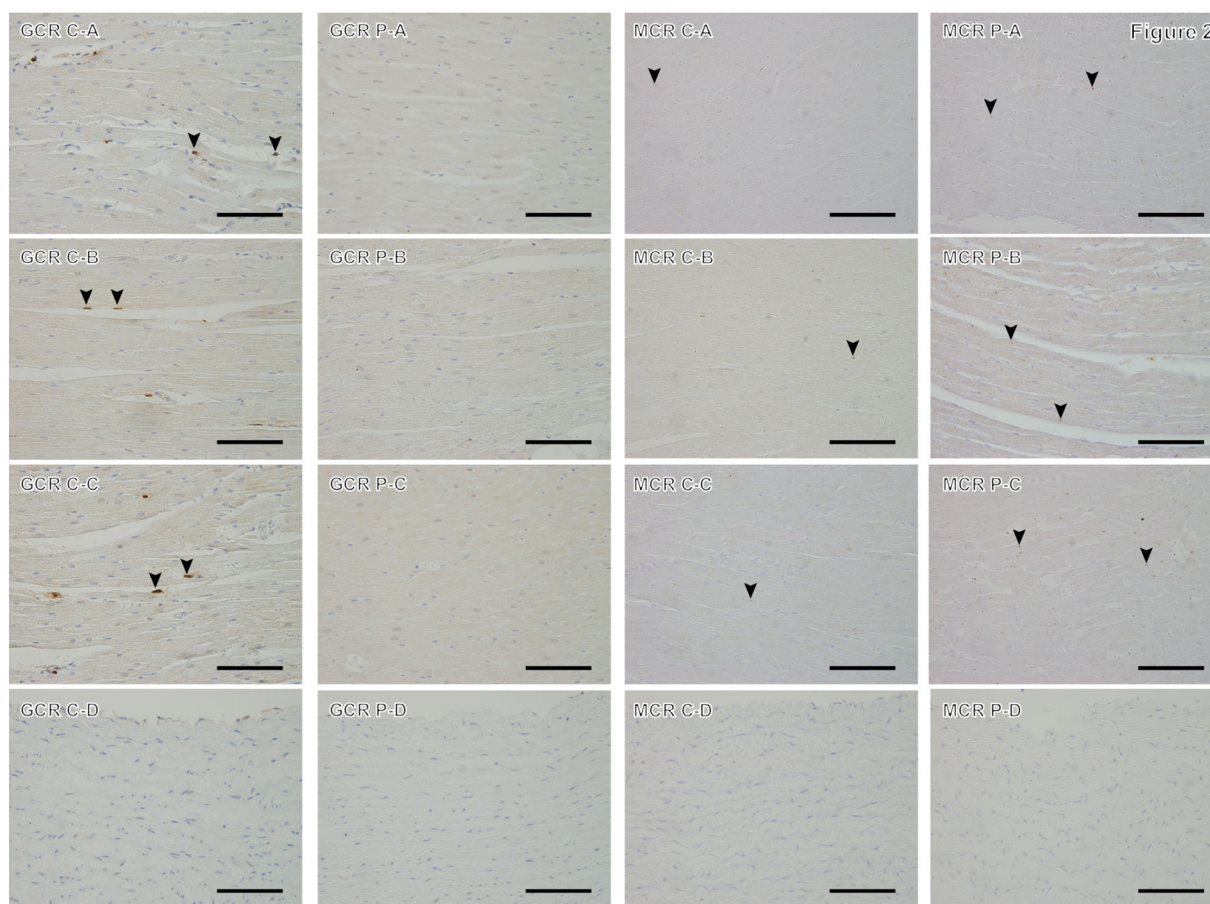
Fig. 2. Immunostaining of glucocorticoid receptor and mineralocorticoid receptor in the control group (C) and high-dose prednisolone group (P). A: Myocardium of the left ventricular wall; B: myocardium of the right ventricular wall; C: interventricular septum; and D: aorta; GCR: anti-glucocorticoid receptor immunostaining; MCR: anti-mineralocorticoid receptor immunostaining. GCR sections in the C group show brown-stained GCR-positive nuclei (arrowheads) and violet-stained negative nuclei. P group does not show any GCR-positive nuclei in the shown fields. MCR sections in the C and P groups' myocardium shows brown-stained MCR immunoreactivity positive points (arrowheads) and violet-stained negative nuclei, whereas there are fewer MCR-positive staining points in group C. For the aorta, both groups showed less immunoreactivity for GCR and MCR. Magnification: 400×, scale bar=50 μm.

fibers in the IVS and LVM on echocardiographic results (Co=0.009; CI=0.004–0.014; $P<0.0001$). Furthermore, there was a significant negative relationship with the percentage of area occupied by collagen fibers in the IVS and Em on the IVS side (Co= −0.107; CI= −0.167– −0.046; P=0.001) and E/Em (Co= −0.018; CI= −0.005– −0.031; P=0.006).

DISCUSSION

Clinical signs, blood biochemistry, and hormone tests observed after the start of the medication suggest that the dogs in the P group could replicate iatrogenic CS [40].

In this study, LVH and decreased LV diastolic function were observed on echocardiography, as recently reported in veterinary medicine [5, 9, 11]. LVH and fibrosis are also caused by systemic hypertension, a common complication in CS [2, 15]. None of the conventional echocardiographic results correlated with SBP, which is consistent with previous reports of no relationship between LVFW thickness and systolic blood pressure in canine CS patients [22, 44].

Functionally, conventional echocardiography revealed a significant increase in the PEP/ET ratio on Day 84, potentially suggesting a reduction in left ventricular systolic function [28]. However, EF and Sm increased on TDI. These results are contradictory, suggesting that HGC did not clearly account for systolic function in this study. Furthermore, conventional echocardiography revealed no abnormalities in the transmitral inflow pattern, whereas TDI showed a reduction in Em on the IVS side. Decreased LV diastolic function is characterized by decreased Em, increased Am, and an Em/Am ratio <1 [36]. Despite no significant increase in Am, the Em/Am ratio was <1 on the IVS side at Day 56 and <1 on the LVFW side at Day 84. Reduced E/A ratio indicate abnormal LV flaccidity, but these changes may be absent or obscure in the early stages of cardiac disease [12]. The IVS side of the mitral annulus is more appropriate for assessing cardiac function than the LVFW side [10]. Taken together, we observed a decline in LV diastolic function at an early-stage, and the decline in Em seen only on the IVS side is a reliable result in

assessing LV diastolic function. Glucocorticoid (GC)-induced hypertension may influence the reduction in velocity of myocardial dilatation, as it negatively correlated with SBP for the reduction in IVS side of Em.

Histopathological examination showed that the percentage of collagen fibers in the LV and IVS was increased in the P group compared with that in the C group. Thus, it was suggested that persistent HGC could cause myocardial fibrosis similar to that observed in human CS [25, 30, 43]. There was a positive relationship between the percentage of area occupied by collagen fibers in the IVS and the results of echocardiography IVSd and LVM, and a significant negative relationship between the percentage of area occupied by collagen fibers in the IVS for IVS side Em. Recently, an increase in perivascular and interstitial fibers in the LV myocardium with DD has been reported in rats treated with GCs compared that in control rats [21]. Besides, fibroblasts involved in myocardial fibrosis are associated with the development of DD and hypertrophy [31]. Therefore, we hypothesized that fibrosis may be one of the causes of the LVH and DD reported in dogs with CS and dogs treated with high doses of prednisolone.

The percentage of GCR immunostaining-positive nuclei in the P group was significantly decreased in the LVFW, RVFW, and IVS compared with that in the C group, and the percentage of MCR immunostaining-positive sites in the P group was significantly increased in the LVFW and RVFW compared with that in the C group. Accordingly, GCR and MCR have also been reported to be expressed in the canine heart [20, 37]. MCR detected in non-epithelial cells, such as cardiomyocytes and aorta, is highly reactive to mineralocorticoids and GCs such as cortisol [1, 18]. Besides, although the affinity of GCs for MCR is similar to that of aldosterone, the concentration of GCs in the blood of dogs is much higher than that of aldosterone [26]. Therefore, for aldosterone to bind and activate MCR, cortisol must be inactivated by cortisone, which has no affinity for MCR. In this regard, 11beta-hydroxysteroid dehydrogenase (11β-HSD) type 1 converts cortisone to its active form, cortisol, whereas 11β-HSD type 2 inactivates cortisol to cortisone [14, 23]. In humans and rodents, MCR is present not only in the kidney but also in the heart and vascular wall, whereas 11β-HSD type 2 is rarely expressed in myocardial tissue [8, 38]. Therefore, both MCR and GCR may mediate the action of GCs in cardiomyocytes.

As reported recently, administration of high doses of GCs (dexamethasone 10^{-6} mol/l) to human umbilical vein endothelial cells downregulated GCR and, in contrast, upregulated MCR expression [46]. Besides, excessive GC exposure is known to cause downregulation of GCR expression [7, 29]. Thus, in the present study, excess GCs may have downregulated GCR, and more GCs bound to MCRs, which were upregulated.

It has also been reported that myocardial fibrosis is mediated by MCR activation, although the detailed mechanisms are not known [2, 6, 47]. Under normal conditions, GCs do not activate MCR; however, it has been reported that under conditions of increased oxidative stress, the GC-MCR complex is activated by reactive oxygen species (ROS) [19, 40]. Although the mechanism of GC-induced hypertension is not fully understood, increased oxidative stress plays a pivotal role in the development of hypertension by causing vasoconstriction, such as through biological inactivation of nitric oxide by the ROS [41, 49]. It has been reported that rats with GC (dexamethasone)-induced hypertension had elevated plasma H_2O_2 concentrations [41]. Reportedly, such oxidative stress activity is increased in rats with GC-induced fibrosis compared with that in control rats [21]. In light of these reports and the fact that SBP at Day 84 in the present study fit the definition of SHT and showed a significant increase compared with that at Day 0, oxidative stress may have increased.

The present study has a few limitations. First, considering the pharmacological difference between cortisol and prednisolone, with prednisolone exhibiting four times stronger GC activity than cortisol [16], the effect of GCs on myocardial tissue may have been more potent than in CS patients with a similar disease progression. However, the impact of LVH and DD in patients with CS has been reported in humans and dogs to progress throughout the disease and be independent of blood cortisol levels, suggesting that its impact is minimal [15, 33]. Second, HGC persists in spontaneous CS, while this model was created by twice-daily prednisolone administration, which may have predicted intermittent increases in blood levels and the duration of steroid hormone exposure to systemic organs may have differed from clinical cases of CS. Third, although the present study did not show a decline in LV systolic function, there may have been a decline in early-stage systolic function if items such as isovolumic acceleration had been examined in more detail. Finally, because this study was conducted in a relatively small population, it may not have the statistical power to detect the effects of synthetic corticosteroids on the heart in a significant manner.

In conclusion, the present study shows that continuous administration of high-dose prednisolone to dogs causes myocardial wall thickening and fibrosis, characterized by increased collagen fibers on the LVFW and IVS. Besides, fibrosis may cause LV hypertrophy and DD in dogs with spontaneous and iatrogenic CS. In dogs with persistent HGC, GCR downregulation was indicated, which affected the development of myocardial fibrosis. However, the detailed mechanisms by which HGC causes myocardial fibrosis remain unclear. Furthermore, additional potential effects on the development of heart failure and cardiovascular complications when the dog's heart is exposed to long-term excessive GCs cannot be ruled out. Therefore, further histological investigations are warranted to elucidate these underlying mechanisms.

REFERENCES

1. Arriza, J. L., Weinberger, C., Cerelli, G., Glaser, T. M., Handelin, B. L., Housman, D. E. and Evans, R. M. 1987. Cloning of human mineralocorticoid receptor complementary DNA: structural and functional kinship with the glucocorticoid receptor. *Science* **237**: 268–275. [Medline] [CrossRef]
2. Azibani, F., Fazal, L., Chatziantoniou, C., Samuel, J. L. and Delcayre, C. 2013. Aldosterone mediates cardiac fibrosis in the setting of hypertension. *Curr. Hypertens. Rep.* **15**: 395–400. [Medline] [CrossRef]
3. Behrend, E. N., Kooistra, H. S., Nelson, R., Reusch, C. E. and Scott-Moncrieff, J. C. 2013. Diagnosis of spontaneous canine hyperadrenocorticism: 2012 ACVIM consensus statement (small animal). *J. Vet. Intern. Med.* **27**: 1292–1304. [Medline] [CrossRef]
4. Boscaro, M., Barzon, L., Fallo, F. and Sonino, N. 2001. Cushing's syndrome. *Lancet* **357**: 783–791. [Medline] [CrossRef]
5. Brown, S., Atkins, C., Bagley, R., Carr, A., Cowgill, L., Davidson, M., Egner, B., Elliott, J., Henik, R., Labato, M., Littman, M., Polzin, D., Ross, L., Snyder, P., Stepien R., American College of Veterinary Internal Medicine. 2007. Guidelines for the identification, evaluation, and management of systemic hypertension in dogs and cats. *J. Vet. Intern. Med.* **21**: 542–558. [Medline] [CrossRef]
6. Buonafine, M., Bonnard, B. and Jaisser, F. 2018. Mineralocorticoid receptor and cardiovascular disease. *Am. J. Hypertens.* **31**: 1165–1174. [Medline] [CrossRef]
7. Campbell, J. E., Király, M. A., Atkinson, D. J., D'souza, A. M., Vranic, M. and Riddell, M. C. 2010. Regular exercise prevents the development of hyperglucocorticoidemia via adaptations in the brain and adrenal glands in male Zucker diabetic fatty rats. *Am. J. Physiol. Regul. Integr. Comp. Physiol.* **299**: R168–R176. [Medline] [CrossRef]
8. Chapman, K., Holmes, M. and Seckl, J. 2013. 11β-hydroxysteroid dehydrogenases: intracellular gate-keepers of tissue glucocorticoid action. *Physiol. Rev.* **93**: 1139–1206. [Medline] [CrossRef]
9. Chen, H. Y., Lien, Y. H. and Huang, H. P. 2014. Assessment of left ventricular function by two-dimensional speckle-tracking echocardiography in small breed dogs with hyperadrenocorticism. *Acta Vet. Scand.* **56**: 88. [Medline] [CrossRef]
10. Chetboul, V., Sampedrano, C. C., Tissier, R., Gouni, V., Saponaro, V., Nicolle, A. P. and Pouchelon, J. L. 2006. Quantitative assessment of velocities of the annulus of the left atrioventricular valve and left ventricular free wall in healthy cats by use of two-dimensional color tissue Doppler imaging. *Am. J. Vet. Res.* **67**: 250–258. [Medline] [CrossRef]
11. Chetboul, V., Tissier, R., Gouni, V., de Almeida, V., Lefebvre, H. P., Concordet, D., Jamet, N., Sampedrano, C. C., Serres, F. and Pouchelon, J. L. 2010. Comparison of Doppler ultrasonography and high-definition oscillometry for blood pressure measurements in healthy awake dogs. *Am. J. Vet. Res.* **71**: 766–772. [Medline] [CrossRef]
12. Choi, J., Kim, H. and Yoon, J. 2013. Pulsed tissue Doppler imaging of the left ventricular septal mitral annulus in healthy dogs. *J. Vet. Sci.* **14**: 85–90. [Medline] [CrossRef]
13. de Bruin, C., Meij, B. P., Kooistra, H. S., Hanson, J. M., Lamberts, S. W. J. and Hofland, L. J. 2009. Cushing's disease in dogs and humans. *Horm. Res.* **71** Suppl 1: 140–143. [Medline]
14. Dube, S., Norby, B. J., Pattan, V., Carter, R. E., Basu, A. and Basu, R. 2015. 11β-hydroxysteroid dehydrogenase types 1 and 2 activity in subcutaneous adipose tissue in humans: implications in obesity and diabetes. *J. Clin. Endocrinol. Metab.* **100**: E70–E76. [Medline] [CrossRef]
15. Fallo, F., Budano, S., Sonino, N., Muiesan, M. L., Agabiti-Rosei, E. and Boscaro, M. 1994. Left ventricular structural characteristics in Cushing's syndrome. *J. Hum. Hypertens.* **8**: 509–513. [Medline]
16. Feldman, E. and Nelson, R. 2003. Canine and Feline Endocrinology and Reproduction, 3rd ed., Saunders, Tokyo.
17. Foppa, M., Duncan, B. B. and Rohde, L. E. 2005. Echocardiography-based left ventricular mass estimation. How should we define hypertrophy? *Cardiovasc. Ultrasound* **3**: 17. [Medline] [CrossRef]
18. Frey, F. J., Odermatt, A. and Frey, B. M. 2004. Glucocorticoid-mediated mineralocorticoid receptor activation and hypertension. *Curr. Opin. Nephrol. Hypertens.* **13**: 451–458. [Medline] [CrossRef]
19. Funder, J. W. 2017. Aldosterone and mineralocorticoid receptors-physiology and pathophysiology. *Int. J. Mol. Sci.* **18**: 1032. [Medline] [CrossRef]
20. Funder, J. W., Duval, D. and Meyer, P. 1973. Cardiac glucocorticoid receptors: the binding of tritiated dexamethasone in rat and dog heart. *Endocrinology* **93**: 1300–1308. [Medline] [CrossRef]
21. Hattori, T., Murase, T., Iwase, E., Takahashi, K., Ohtake, M., Tsuboi, K., Ohtake, M., Miyachi, M., Murohara, T. and Nagata, K. 2013. Glucocorticoid-induced hypertension and cardiac injury: effects of mineralocorticoid and glucocorticoid receptor antagonism. *Nagoya J. Med. Sci.* **75**: 81–92. [Medline]
22. Oui, H., Jeon, S., Lee, G., Park, S., Cho, K. O. and Choi, J. 2015. Tissue Doppler and strain imaging of left ventricle in Beagle dogs with iatrogenic hypercortisolism. *J. Vet. Sci.* **16**: 357–365. [Medline] [CrossRef]
23. Hollis, G. and Huber, R. 2011. 11β-Hydroxysteroid dehydrogenase type 1 inhibition in type 2 diabetes mellitus. *Diabetes Obes. Metab.* **13**: 1–6. [Medline] [CrossRef]
24. Isidori, A. M., Graziadio, C., Paragliola, R. M., Cozzolino, A., Ambrogio, A. G., Colao, A., Corsello, S. M., Pivonello R., ABC Study Group 2015. The hypertension of Cushing's syndrome: controversies in the pathophysiology and focus on cardiovascular complications. *J. Hypertens.* **33**: 44–60. [Medline] [CrossRef]
25. Iwasaki, H. 2014. Reversible alterations in cardiac morphology and functions in a patient with Cushing's syndrome. *Endocrinol. Diabetes Metab. Case Rep.* **2014**: 140038. [Medline]
26. Javadi, S., Galac, S., Boer, P., Robben, J. H., Teske, E. and Kooistra, H. S. 2006. Aldosterone-to-renin and cortisol-to-adrenocorticotropic hormone ratios in healthy dogs and dogs with primary hypoadrenocorticism. *J. Vet. Intern. Med.* **20**: 556–561. [Medline] [CrossRef]
27. Kohara, Y., Soeta, S., Izu, Y. and Amasaki, H. 2015. Accumulation of type VI collagen in the primary osteon of the rat femur during postnatal development. *J. Anat.* **226**: 478–488. [Medline] [CrossRef]
28. Lee, B. H., Dukes-McEwan, J., French, A. T. and Corcoran, B. M. 2002. Evaluation of a novel doppler index of combined systolic and diastolic myocardial performance in Newfoundland dogs with familial prevalence of dilated cardiomyopathy. *Vet. Radiol. Ultrasound* **43**: 154–165. [Medline] [CrossRef]
29. Lipworth, B. J. 2000. Therapeutic implications of non-genomic glucocorticoid activity. *Lancet* **356**: 87–89. [Medline] [CrossRef]
30. Ma, R. C. W., So, W. Y., Tong, P. C. Y., Chan, J. C. N., Cockram, C. S. and Chow, C. C. 2011. Adiposity of the heart revisited: reversal of dilated cardiomyopathy in a patient with Cushing's syndrome. *Int. J. Cardiol.* **151**: e22–e23. [Medline] [CrossRef]
31. Manabe, I., Shindo, T. and Nagai, R. 2002. Gene expression in fibroblasts and fibrosis: involvement in cardiac hypertrophy. *Circ. Res.* **91**: 1103–1113. [Medline] [CrossRef]
32. Masters, A. K., Berger, D. J., Ware, W. A., Langenfeld, N. R., Coetzee, J. F., Mochel, J. P. M. and Ward, J. L. 2018. Effects of short-term anti-inflammatory glucocorticoid treatment on clinicopathologic, echocardiographic, and hemodynamic variables in systemically healthy dogs. *Am. J.*

Vet. Res. **79**: 411–423. [Medline] [CrossRef]

33. Muiesan, M. L., Lupia, M., Salvetti, M., Grigoletto, C., Sonino, N., Boscaro, M., Rosei, E. A., Mantero, F. and Fallo, F. 2003. Left ventricular structural and functional characteristics in Cushing's syndrome. *J. Am. Coll. Cardiol.* **41**: 2275–2279. [Medline] [CrossRef]

34. Nieman, L. K. 2015. Cushing's syndrome: update on signs, symptoms and biochemical screening. *Eur. J. Endocrinol.* **173**: M33–M38. [Medline] [CrossRef]

35. Nivy, R., Refsal, K. R., Ariel, E., Kuzi, S., Yas-Natan, E. and Mazaki-Tovi, M. 2018. The interpretive contribution of the baseline serum cortisol concentration of the ACTH stimulation test in the diagnosis of pituitary dependent hyperadrenocorticism in dogs. *J. Vet. Intern. Med.* **32**: 1897–1902. [Medline] [CrossRef]

36. Oyama, M. A., Sisson, D. D., Bulmer, B. J. and Constable, P. D. 2004. Echocardiographic estimation of mean left atrial pressure in a canine model of acute mitral valve insufficiency. *J. Vet. Intern. Med.* **18**: 667–672. [Medline] [CrossRef]

37. Reynoso Palomar, A. R., Rodriguez Bravo, M., Villa Mancera, A. E. and Mucha, C. J. 2017. Expression and biochemical characteristics of two different aldosterone receptors in both healthy and dilated cardiomyopathy dog heart tissue. *Vet. Res. Commun.* **41**: 9–14. [Medline] [CrossRef]

38. Richardson, R. V., Batchen, E. J., Thomson, A. J. W., Darroch, R., Pan, X., Rog-Zielinska, E. A., Wyrzykowska, W., Scullion, K., Al-Dujaili, E. A. S., Diaz, M. E., Moran, C. M., Kenyon, C. J., Gray, G. A. and Chapman, K. E. 2017. Glucocorticoid receptor alters isovolumetric contraction and restrains cardiac fibrosis. *J. Endocrinol.* **232**: 437–450. [Medline] [CrossRef]

39. Rishniw, M. and Erb, H. N. 2000. Evaluation of four 2-dimensional echocardiographic methods of assessing left atrial size in dogs. *J. Vet. Intern. Med.* **14**: 429–435. [Medline] [CrossRef]

40. Rossier, M. F., Python, M. and Maturana, A. D. 2010. Contribution of mineralocorticoid and glucocorticoid receptors to the chronotropic and hypertrophic actions of aldosterone in neonatal rat ventricular myocytes. *Endocrinology* **151**: 2777–2787. [Medline] [CrossRef]

41. Safaeian, L., Hajhashemi, V., Haghjoo Javanmard, S. and Sanaye Naderi, H. 2016. The effect of protocatechuic acid on blood pressure and oxidative stress in glucocorticoid-induced hypertension in rat. *Iran. J. Pharm. Res.* **15** Suppl: 83–91. [Medline]

42. Sahn, D. J., DeMaria, A., Kisslo, J. and Weyman, A. 1978. Recommendations regarding quantitation in M-mode echocardiography: results of a survey of echocardiographic measurements. *Circulation* **58**: 1072–1083. [Medline] [CrossRef]

43. Sugihara, N., Shimizu, M., Kita, Y., Shimizu, K., Ino, H., Miyamori, I., Nakabayashi, H. and Takeda, R. 1992. Cardiac characteristics and postoperative courses in Cushing's syndrome. *Am. J. Cardiol.* **69**: 1475–1480. [Medline] [CrossRef]

44. Takano, H., Kokubu, A., Sugimoto, K., Sunahara, H., Aoki, T. and Fijii, Y. 2015. Left ventricular structural and functional abnormalities in dogs with hyperadrenocorticism. *J. Vet. Cardiol.* **17**: 173–181. [Medline] [CrossRef]

45. Tinklenberg, R. L., Murphy, S. D., Mochel, J. P., Seo, Y. J., Mahaffey, A. L., Yan, Y. and Ward, J. L. 2020. Evaluation of dose-response effects of short-term oral prednisone administration on clinicopathologic and hemodynamic variables in healthy dogs. *Am. J. Vet. Res.* **81**: 317–325. [Medline] [CrossRef]

46. Wang, X. Y., Chen, X. L., Wang, L. and Chen, H. W. 2015. High-dose glucocorticoids increases the expression of mineralocorticoid receptor in vascular endothelial cells. *Eur. Rev. Med. Pharmacol. Sci.* **19**: 4314–4323. [Medline]

47. Qin, W., Rudolph, A. E., Bond, B. R., Rocha, R., Blomme, E. A., Goellner, J. J., Funder, J. W. and McMahon, E. G. 2003. Transgenic model of aldosterone-driven cardiac hypertrophy and heart failure. *Circ. Res.* **93**: 69–76. [Medline] [CrossRef]

48. Wess, G., Killich, M. and Hartmann, K. 2010. Comparison of pulsed wave and color Doppler myocardial velocity imaging in healthy dogs. *J. Vet. Intern. Med.* **24**: 360–366. [Medline] [CrossRef]

49. Wilcox, C. S. 2002. Reactive oxygen species: roles in blood pressure and kidney function. *Curr. Hypertens. Rep.* **4**: 160–166. [Medline] [CrossRef]